C.P. No. 408
(20,204)
A.R.C Technical Report

C.P. No. 408
(20,204)
A.R.C Technical Report

MINISTRY OF SUPPLY

AERONAUTICAL RESEARCH COUNCIL

CURRENT PAPERS

Some Notes on the Use of Resistance Thermometers for the Measurement of Heat Transfer Rates in Shock Tubes

by

B. D. Henshall, B.Sc., Ph.D., and

D. L. Schultz, B.E., D. Phil.,

of the Aerodynamics Division, N.P.L.

LONDON: HER MAJESTY'S STATIONERY OFFICE

1959

Price 3s 6d net

Current Paper No. 408

Some Notes on the Use of Resistance Thermometers for the Measurement of Heat Transfer Rates in Shock Tubes.

Erratum

Page 11 Lower R.H. Table. $\sec^{-\frac{1}{2}}$ *should read* $\sec^{\frac{1}{2}}$

Aeronautical Research Council
May 1959

London: Her Majesty's Stationery Office

DS 44853/1/Wt.52 K.4 6/59 R

C.P. No. 4[illegible]8

Some Notes on the Use of Resistance Thermometers for the Measurement of Heat Transfer Rates in Shock Tubes

- By -
B. D. Henshall, B.Sc., Ph.D.
and
D. L. Schultz, B.E., D.Phil.,
of the Aerodynamics Division, N.P.L.

29th May, 1958

SUMMARY

A brief description is given of the model calibration technique, and the experimental data reduction employed at the N.P.L. in the determination of heat transfer rates in a hypersonic shock tube. Estimates are made of the probable accuracy of such measurements, and specimen calculations and results are given.

---

1. Introduction

At the present time there is considerable interest in the determination of the heat transfer rates experienced by vehicles re-entering the earth's atmosphere at hypersonic speeds. One experimental facility in which simulation of the re-entry problem is possible is the hypersonic shock tube[1]: but the duration of the high stagnation temperature hypersonic flow is only of the order of 100 microseconds, and thus any experimental instrumentation must have a response time of the order of 1 microsecond or less to enable the details of the flow to be investigated.

The thin film resistance thermometer is an instrument with a response time considerably less than 0.1 microsecond[2], and is ideally suited to the measurement of transient surface temperatures from which the heat transfer rates may be deduced.

2. Manufacture of Heat Transfer Gauges

Thin film resistance thermometers may be made in various ways, but in every case a thin metallic film is applied to an insulator which is usually soda glass, pyrex or quartz. Such films may be applied by sputtering[3], evaporation[4] or painting[5,7] and baking on to the insulator; at the N.P.L. the simplest technique has been adopted, and painted films of Hanovia 05 Liquid Bright Platinum* are used. The liquid, a suspension of platinum and silver in oil of lavender, is applied by hand with a small brush, air dried, and subsequently baked. During the baking process the solvent evaporates, and a thin metal film is left on the model. Although the uniformity of the film thickness and area obtained by painting is inferior to that obtained by the other methods, the painted films are exceptionally robust, and are greatly superior to the other types for use

in/

---

*Manufactured by Hanovia Products Ltd., 52, High Holborn, London, W.C.1.

in shock tubes at high shock speeds and high flow densities. With practice, the painted films have very reproducible physical properties. At N.P.L. we have found that the most durable films are produced when the baking temperature of a well-ventilated oven is as near as possible to the softening point of the glass backing material. The temperature of the oven is increased to a maximum value in approximately 30 minutes, and then held there for an equal time. Pyrex glass models are baked at 600°C, and soda glass models at 580°C. The electrical leads to the resistance thermometer are attached by using low-melting point flux-cored silver alloy solder**. A typical stagnation-point model is shown in Fig.1; the resistance of the element is about 50 ohms.

Resistance thermometers, by virtue of their exceptionally fast response time, are excellent shock wave detectors, and are the standard instrument at N.P.L. for this purpose. The output from each gauge is amplified, and triggers a hydrogen thyratron which produces a marker pip: alternatively the output of the gauge may be displayed directly. These 'wall' resistance thermometers consist of a painted film about 4 mm × 0.5 mm applied to the end of a pyrex glass rod, which is mounted with the end flush with the wall of the shock tube. The film is connected to the current supply via thick painted leads*** down the sides of the rod. The resistance of the thermometer element is about 30 ohms, and that of the painted leads effectively zero.

3. The Output of a Resistance Thermometer

The time taken t_d for thermal waves to diffuse through the thin film resistance thermometer of typical thickness δ is given[3] by×

$$t_d = \left(\frac{\rho_f \, c_f}{K_f} \right) \delta^2$$

where ρ_f, c_f and K_f are respectively the density, specific heat and thermal conductivity of the film material. Thus for a painted platinum film of thickness 10^{-4} cm the diffusion time t_d is about 10^{-10} sec+. Since the running time of the shock tube is much longer than this, the film is acting as a true surface resistance thermometer: the temperature of the film is uniform, and equal to the instantaneous surface temperature of the backing material during the running time of the shock tube. It may be noted that the backing material need only be 1 mm thick in order to act as a semi-infinite solid heat sink with respect to the thin film resistance thermometer.

A constant current I_o is supplied to the resistance thermometer of resistance R_o giving a voltage drop E_{f_o} across the film. At the N.P.L. we standardise E_{f_o} as 1.0V for all films, and usually $R_o \sim 50$ ohms and $I_o \sim 20$ milliamperes. Under these conditions the heating $I_o^2 R_o \sim 0.02$ watts/cm^2, whereas the heat transfer rates in the running time of the shock tube are ~ 1000 watts/cm^2. During an experiment the

temperature/

**L.M.P. 2% silver, M.P.179°C, 362 flux. Manufactured by Multicore Solders Ltd., Hemel Hempstead, Hertfordshire.

***Silver paste X 351 (flux) X 353 (coat) from Johnson Matthey Ltd., 73-83 Hatton Garden, London.

×For notation, see Appendix.

+This is very much shorter than the resolving power of any currently available electronic recording equipment.

temperature rise of the film appears as a voltage variation across the film, since the current flowing through the film is constant. Then the voltage rise ΔE is given by

$$\Delta E = I_o \Delta R_o, \qquad \text{where} \quad \Delta R_o = R_o \alpha \Delta T_o, \qquad \ldots(1)$$

and α is the temperature coefficient of resistivity. The required relation between the surface heat transfer rate and the experimentally determined temperature change of the film is obtained by solving the classical one-dimensional heat conduction equation, with the appropriate boundary conditions. Comprehensive problems are solved in Ref.6, and the shock tube problem is treated in detail in Ref.2. The relevant solutions are quoted below:-

Shock Tube: Constant Heat Transfer Rate $\dot{q}$; Surface Temperature T

$$\dot{q} = \frac{4.19\sqrt{\pi}}{2E_{f_o}} \left(\frac{\sqrt{\rho cK}}{\alpha}\right)\left(\frac{E(t)}{\sqrt{t}}\right) \qquad \ldots(2)$$

$$T = \frac{2\dot{q}}{\sqrt{\pi}} \sqrt{\frac{t}{\rho cK}} \qquad \ldots(3)$$

Shock Tube: Non-constant Heat Transfer Rate $\dot{q}(t)$; Surface Temperature $T(t)$

$$\dot{q}(t) = \frac{4.19}{2\sqrt{\pi}\, E_{f_o}} \left(\frac{\sqrt{\rho cK}}{\alpha}\right)\left\{\frac{2E(t)}{\sqrt{t}} + \int_o^t \frac{E(t)-E(\tau)}{(t-\tau)^{\frac{1}{2}}}\, d\tau\right\} \qquad \ldots(4)$$

$$T(t) = \frac{1}{\sqrt{\pi}\sqrt{\rho cK}} \int_o^t \frac{q(\tau)}{(t-\tau)^{\frac{1}{2}}}\, d\tau. \qquad \ldots(5)$$

In the above equations ρ, c and K are respectively the density, specific heat and the thermal conductivity of the backing material. The experimental result gives the voltage across the film as a function of time, and thus we can calculate the heat transfer rate $\dot{q}$ from (2) or (4), provided the 'calibration constant' $\left(\frac{\alpha}{\sqrt{\rho cK}}\right)$ is known.

The use of equations (2) and (4) will be illustrated later when the meaning of the integration variable τ will become clear.

We must next consider the determination of the physical properties of the resistance thermometer; clearly, the 'calibration constant' $\left(\frac{\alpha}{\sqrt{\rho cK}}\right)$ determines the sensitivity of the thin film resistance thermometer, and it is apparent from equation (2) that this quantity should be as large as possible. This may be achieved by using pure metals as resistance elements, and poor conductors as the backing material. The temperature coefficient of resistance α appropriate to the bulk material is not achieved in very thin films[8,9], but there is evidence to show that for a film which adheres firmly to the backing material the bulk properties (ρcK) of the insulator may be used with good accuracy. Table 1 gives handbook values of α, $\sqrt{\rho cK}$ and $\left(\frac{\alpha}{\sqrt{\rho cK}}\right)$ for several common materials. Later we will note that the experimentally determined values of $\left(\frac{\alpha}{\sqrt{\rho cK}}\right)$ agree reasonably well with

the/

the tabulated values. There is no apparent reason why the new cermets should not be used as backing materials; indeed, their high thermal conductivity (0.04 → 0.07 cal/cm °C sec) may prove useful under the extreme conditions encountered at high shock speeds where glass models appear to spall badly, and a new model is required for each run. The value of $\left(\frac{\alpha}{\sqrt{\rho c K}}\right)$ for a cermet model would not be so unreasonably low that the sensitivity suffered.

4. The Calibration of a Resistance Thermometer

The calibration is performed by applying a constant heat transfer rate to the thin film resistance thermometer which is located in one arm of a Wheatstone Bridge as illustrated in Fig.2.

As the film of resistance R_o is heated by the discharge of the capacitor C at a constant current I_o the power dissipated is $I_o^2 R_o$ watts in the film, and an out-of-balance voltage appears across the bridge. This is displayed on an oscilloscope and photographed. In the N.P.L. calibration circuit shown in Fig.2, the capacitor C is 200 μF and the time constant of the discharge is approximately 0.1 sec. This is much greater (200 times) than the time interval used to determine $\left(\frac{\alpha}{\sqrt{\rho c K}}\right)$ - usually 500 microseconds - in order to preserve a truly constant heat transfer rate[3], and therefore an exact simulation of the conditions produced by the shock tube. Figs. 2 and 3 show how each model is calibrated by this technique. The oscilloscope record of Fig.3(a) is enlarged and traced as Fig.3(c): photographs of the model and a ruler under identical magnifications appear in Fig.3(b). The area of the resistance thermometer is deduced from planimeter measurements of tracings of the model area and the scale. The errors involved in the determination of the element area by this procedure are estimated at ±5% from repeated measurements of the same model film by different operators.

Now equation (2) shows that for a constant heat transfer rate the voltage variation with time is parabolic, hence a simple deduction from the oscilloscope trace of $V(t)$ against t (Fig.3(c)) gives $V^2(t)$ against t (Fig.3(d)) which is always found to be a straight line. The initial transients are seen to decay after 40 → 50 microseconds. With the bridge circuit as shown in Fig.2, and noting that $R_1 = R_2 = R_3$, we can easily show that the out-of-balance voltage ΔV is given by

$$\frac{\Delta V}{I_o} = \frac{R_2 \, \Delta R_o}{(R_o + \Delta R_o + R_2)}, \qquad \ldots(6)$$

whence

$$\Delta R_o = \frac{\frac{\Delta V}{I_o}(R_o + R_2)}{R_2 - \frac{\Delta V}{I_o}}. \qquad \ldots(7)$$

Now

$$\dot{q} = \frac{I_o^2 R_o}{4.19A} \text{ cals/sec/cm}^2 \qquad \ldots(8)$$

and

$$I_o = \frac{V}{\left[R_o + R_2 + R_s\left\{\frac{R_o + 3R_2}{2R_2}\right\}\right]}. \qquad \ldots(9)$$

Further,/

Further, from (1) and (3)

$$\dot{q} = \frac{\sqrt{\pi}}{2}\sqrt{\frac{\rho c K}{t}}\,.\,\Delta T_o = \frac{\sqrt{\pi}}{2}\,\frac{\sqrt{\rho c K}}{\alpha R_o}\,\frac{\Delta R_o}{\sqrt{t}} \text{ cals/sec/cm}^2. \qquad \ldots(10)$$

On rearrangement (10) becomes with (8)

$$\frac{\alpha}{\sqrt{\rho c K}} = \frac{A.\sqrt{\pi}}{2}\,\frac{4.19}{I_o^2 R_o^2}\,\frac{\Delta R_o}{\sqrt{t}}\,\frac{\sec^{\frac{1}{2}}}{\text{cals}} \text{ cm}^2. \qquad \ldots(11)$$

It is found that ΔV is typically 1 volt, which is small compared with $V \sim 250$ volts. Then (7) becomes $\Delta R_o = \frac{\Delta V}{I_o}\left(\frac{(R_o + R_2)}{R_2}\right)$. $\qquad \ldots(12)$

Finally, combining (11) and (12) with (9) we get

$$\frac{\alpha}{\sqrt{\rho c K}} = \left[\frac{A.4.19\sqrt{\pi}}{2V^3}\right]\left[\frac{\Delta V}{\sqrt{t}}\right]\left[\frac{(R_o+R_2)}{R_o^2 R_2}\right]\left[R_o + R_2 + \left(\frac{R_o+3R_2}{2R_2}\right)R_s\right]^3 \text{cm}^2\ \sec^{\frac{1}{2}}\ \text{cals}^{-1}. \qquad \ldots(13)$$

Thus the bridge method obtains the calibration constant $\frac{\alpha}{\sqrt{\rho c K}}$ directly, and there is no need to determine α by a separate experiment, unless we wish to find the variation of surface temperature T with time. Normally we are only concerned with the heat transfer rate $\dot{q}$. The values of $\frac{\alpha}{\sqrt{\rho c K}}$ obtained at N.P.L. vary from 0.02 to 0.07 and agree with the measurements of Ref.3 and the values in Table 1. Any model which has a value outside this range is discarded: over 85% of all models fall within the range quoted. The various quantities of equation (13) may be easily measured to 1% with the exception of the slope $\Delta V/\sqrt{t}$ from the reduction of the oscilloscope record. In this value an error of ±3% is likely, and so the values of $\frac{\alpha}{\sqrt{\rho c K}}$ are accurate to ±5% overall. This has been checked by calibrating a given model several times in succession.

5. Reduction of Experimental Data

Before giving a worked example of the graphical integration of equation (4), it is instructive to show that equation (4) reduces to equation (2) for the special case of a constant heat transfer rate. Such a special case is the parabola through the origin given by

$$E(\tau) = E(t)\,\frac{\tau^{\frac{1}{2}}}{t^{\frac{1}{2}}}. \qquad \ldots(14)$$

We must note that the nomenclature of equation (4) means that we wish to evaluate a point heat transfer rate $\dot{q}(t)$ at time t, whereas the experimental result gives the voltage output $E(\tau)$ as a function of time τ. Thus equation (4) implies that the point heat transfer rate $\dot{q}(t)$ depends on the surface temperature at all times τ less than $\tau = t$.

Now/

Now (4) can be written

$$\dot{q}(t) = \text{constant}\left\{\frac{2(E(t))}{\sqrt{t}} + \int_0^t \frac{E(t)-E(\tau)}{(t-\tau)^{\frac{3}{2}}}\,d\tau\right\}, \qquad \ldots(15)$$

and, using (14), we get

$$\dot{q}(t) = \text{constant}\left\{1 + \frac{1}{2}\int_0^t \frac{t^{\frac{1}{2}}\left(1 - \frac{\tau^{\frac{1}{2}}}{t^{\frac{1}{2}}}\right)d\tau}{t^{\frac{3}{2}}\left(1 - \frac{\tau}{t}\right)^{\frac{3}{2}}}\right\}, \qquad \ldots(16)$$

where the constant $C = \dfrac{2E(t)}{\sqrt{t}}\left(\dfrac{\sqrt{\rho cK}}{\alpha}\right)\dfrac{4.19}{2\sqrt{\pi}.E_{f_o}}$. $\qquad \ldots(17)$

In (16) put $\tau = t\sin^2\theta$, and perform the integration. Then we have

$$\dot{q}(t) = C\left\{1 + \int_0^{\pi/2} d(\sec\theta) - \int_0^{\pi/2} d(\tan\theta) + \int_0^{\pi/2} d\theta\right\}$$

$$= C.\frac{\pi}{2}$$

$$= \frac{4.19\sqrt{\pi}}{2E_{f_o}}\left(\frac{\sqrt{\rho cK}}{\alpha}\right)\frac{E(t)}{\sqrt{t}}$$

which is equation (2).

Worked Example

Run 273 has been chosen to illustrate the data reduction method used at the N.P.L. In Run 273 a stagnation point heat transfer rate measurement was made using Model 26. The model was situated in the straight channel about 16 ft from the diaphragm of the N.P.L. 3 inch Hypersonic Shock Tunnel. The initial pressure p_1 in the channel was 3 mm of mercury and the shock Mach number M_s just upstream of the model was measured to be 8.3. Full details of shock speed and 'running-time' measurements, stagnation point heat transfer measurements and a wall boundary layer investigation are given in other papers now in preparation.

(a) Constant heat transfer rate analysis - Eqn. (2)

The oscilloscope record Fig.4(a) is enlarged and traced on graph paper as in Fig.4(b). The ordinates of Fig.4(b) are squared, and plotted against the same abscissa in Fig.4(c). The time is measured from the instant the shock wave strikes the model; this is clearly indicated on the oscilloscope trace (Fig.4(a)).

If the heat transfer is constant during the running time of the shock tube - in this run the contact surface arrives at approx 165 microseconds after the shock wave - Fig.4(c) should be a straight line. This is indeed the case, and thus an analysis of the instantaneous heat transfer rates at any time t from $\tau = 0$ to 165 microseconds should give the same value as this constant heat transfer analysis; viz., 1.65 Kw/cm^2, from equation (2), using the model constants and the experimentally determined slope $E/\sqrt{t}$.

(b)/

(b) Instantaneous heat transfer rate analysis - Eqn. (4)

Table 2 shows how the calculation is made of the point heat transfer rate at a time $t = 150$ microseconds in Run 273. The quantity $\left\{\frac{E(t) - E(\tau)}{(t-\tau)^{\frac{1}{2}}}\right\}$ has to be integrated graphically after it has been tabulated and plotted for all values of τ between 0 and $\tau = t$ (= 150 microseconds in this case). The plotted curve is given in Fig.4(d). Although the ordinate approaches the value 0/0 as $\tau \to t$, it can be shown[5] that

$$\frac{E(t) - E(\tau)}{(t-\tau)^{\frac{1}{2}}} \to 0 \quad \text{as} \quad t \to \tau,$$

and thus any errors in this graphical integration probably arise from the region where $\tau \doteqdot t$. At N.P.L. we adopt the procedure shown in Fig.4(d), and draw a triangle (shaded) whose area is added to the area under the curve. The curve is stopped short at the position $\tau = 95\%t$ in most cases. Equation (4) is then applied, and the instantaneous heat transfer rate deduced. Four calculations were made for Run 273: the constant heat transfer analysis gave $\dot{q} = 1.65$ Kw/cm^2 and the instantaneous heat transfer rate analysis gave

$$\dot{q} = 1.67 \quad 1.62 \text{ and } 1.71 \text{ Kw/cm}^2$$

$$\text{at} \quad t = 50, 100 \text{ and } 150 \text{ microseconds respectively.}$$

Errors made in the integration are probably ±10%, but it should be noted that equation (4) is relatively insensitive to the value of the integral term; the term $2.E(t)/\sqrt{t}$ is usually 2 or 3 times the value of the integral term.

When tracing the oscilloscope record, the operator endeavours to follow the centre of the trace; the errors induced by drawing two separate curves at the extremities of the line width are shown in Fig.4(e). It is clearly shown that these errors are not significant; the errors arise from errors in the slope of the curve.

6. Summary of Experimental Errors

(a) Determination of model constants $\left(\frac{\alpha}{\sqrt{\rho c K}}\right)$ and Area A.

These are both ±5%.

(b) Determination of the voltage drop across the film E_{f_o}.

This is certainly less than ±1%.

(c) Determination of the quantity $E(t)/\sqrt{t}$ and the graphical integration.

Error in $E(t)/\sqrt{t}$ is ±3%

Error in integration ±10%.

Thus the probable error in a value of $\dot{q}$ obtained from equation (2) is

$$\pm\sqrt{\left(\frac{1}{100}\right)^2 + \left(\frac{5}{100}\right)^2 + \left(\frac{3}{100}\right)^2} = \underline{\pm 6\%}.$$

The probable error in a value of $\dot{q}$ from equation (4) is

$$\pm\sqrt{\left(\frac{1}{100}\right)^2 + \left(\frac{5}{100}\right)^2 + \left(\frac{7}{100}\right)^2} = \underline{\pm 8\tfrac{1}{2}\%}.$$

Thus/

Thus the errors in the measurement of the heat transfer rates have been evaluated. However, other errors occur in measuring the initial pressure in the channel of the shock tube, and the effective shock Mach number applicable to the experiment. The channel pressure is usually of the order of a few millimetres of mercury and the probable error is about ±5%, if allowance is made for any possible changes between reading the pressure and firing the shock tube. A much more serious error can arise in the measurement of shock Mach number. A detailed investigation of shock speed measurements made in the 3" shock tube at N.P.L. will be reported shortly; however, it is clear that the shock Mach number should be measured at closely spaced intervals just upstream of the model under test and, even then, the extrapolation to the model may cause considerable error. With the present limited number of instrumentation ports on the N.P.L. 3" shock tube, it is considered that errors of ±10% in the 'effective' shock Mach number could be made. These errors will apply equally to heat transfer rate measurements in the unexpanded or expanded flow of a hypersonic shock tube, and they appear as uncertainties in the precise value of the simulated flight velocity. In the expanded flow case, further errors must arise from possible non-equilibrium effects in the nozzle flow processes (as yet undetermined), and from difficulties in the determination of the flow Mach number and hence the simulated altitude of the experiment. In an unexpanded flow experiment, the effective altitude (i.e., density) is known to the accuracy of measurement of the initial channel pressure, but in the expansion it is probable that simulated altitudes may be in error by ±20%.

Therefore we believe the heat transfer rate itself to be in error by ±10% in unexpanded or expanded shock tube flow; but errors in the simulated altitude for a given run will be different in the two cases whilst errors in the simulated velocity will be the same in both cases. Thus we feel that heat transfer rate measurements made at N.P.L. to date and stated as $\dot{q}$ Kw/cm^2 at U ft/sec at h feet altitude are subject to overall errors of ±20% in the unexpanded flow and about ±40% in the expanded flow of the 3" N.P.L. hypersonic shock tube.

7. Conclusions

A brief description is given of the model calibration technique and the experimental data reduction employed at the N.P.L. in the determination of heat transfer rates in shock tubes.

The probable accuracy of such measurements in the unexpanded flow was estimated at ±20% and in the expanded flow at ±40%. Specimen calculations showed that both the constant and instantaneous heat transfer rate analyses gave similar results when applied to a specific run in the unexpanded flow where the heat transfer rate was known to be constant.

Acknowledgements

Mr. P. S. Pusey assisted in the experimental work and Mrs. N. A. North performed most of the data reduction.

References/

References

No.	Author(s)	Title, etc.
1	D. L. Schultz and B. D. Henshall	Hypersonic shock tube equipment at the National Physical Laboratory, U.K. NATO AGARD Report 147, July, 1957.
2	R. Bromberg	Use of the shock tube wall boundary layer in heat transfer studies. Jet Propulsion Vol.26 No.9, p.737. September, 1956.
3	J. Rabinowicz, M. E. Jessey and C. A. Bartsch	Resistance thermometer for heat transfer measurement in a shock tube. CALCIT Memo No.33, July, 1956.
4	V. H. Blackman	Vibrational relaxation in O_2 and N_2. Princeton University Report NR061-20, May, 1955.
5	R. J. Vidal	A resistance thermometer for transient surface temperature measurements. Paper presented at the American Rocket Society meeting in Buffalo, N.Y. September 24-26, 1956.
6	H. S. Carslaw and J. C. Jaeger	Conduction of heat in solids. Oxford Clarendon Press. 1947.
7	P. H. Rose and F. R. Riddell	An investigation of stagnation point heat transfer in dissociated air. AVCO Research Report 7, April, 1957.
8	L. Holland	Vacuum deposition of thin films. Chapman and Hall, 1956.
9	C. C. Winding, L. Topper and B. V. Daus	Metal-film resistance thermometers for measuring surface temperatures. Indust. and Eng. Chemistry 47, 3, 1955 pp.386-392.
10	D. E. Gray (Ed)	American Institute of Physics Handbook. McGraw-Hill Book Co. Inc. New York, 1957.
11	O. W. Eshbach (Ed)	Handbook of Engineering Fundamentals. John Wiley and Son Inc. New York, 1945.

APPENDIX/

APPENDIX

Notation

a_1	speed of sound ahead of incident shock
A	area of thin film resistance thermometer, sq cm
C	capacity
c	specific heat cal/gm. °C
E	voltage (shock tube experiment)
h	altitude, feet
I	current, amp
K	thermal conductivity cal/cm. °C sec
M_{s_1}	shock Mach number = (velocity of shock)/a_1
p_1	initial pressure in channel of shock tube
R	resistance, ohms
$\dot{q}$	heat transfer rate watts/cm^2
T	temperature, °C
t or τ	time
U	velocity ft/sec
V	voltage (calibration procedure)
α	temperature coefficient of resistance $(°C)^{-1}$
δ	thickness of film
ρ	density gm/cm^3
Δ	denotes small changes in a quantity

Subscripts

$(\ )_o$	initial conditions of film
$(\ )_f$	refers to film material

Table 1/

Table 1

Handbook Properties of Thin Film Resistance Thermometers

(from References 10 and 11)

Insulating Backing Material	Density ρ $\frac{gm}{cm^3}$	Specific Heat C $\frac{cal}{gm\ ^\circ C}$	Thermal Conductivity K $\frac{cal}{cm\ ^\circ C\ sec}$	$\sqrt{\rho cK}$ $\frac{cals}{^\circ C\ cm^2\ sec^{1/2}}$
Soda glass	2.59	0.161	0.00172	0.0266
Pyrex	2.32	0.174	0.00270	0.0330
Porcelain	2.40	0.260	0.00250	0.0395
Quartz	2.65	0.170	0.00352	0.0398

Film Material	Temperature Coefficient of Resistance α $(^\circ C)^{-1}$
Platinum	0.003
Aluminium	0.004
Gold	0.0034
Nickel	0.0054
Nichrome (80-20)	0.000094

Combination	$\frac{\alpha}{\sqrt{\rho cK}}\left(\frac{sec^{-\frac{1}{2}}}{cals}\right)$ per unit area
Platinum-Pyrex	0.091
Platinum-Soda Glass	0.115
Nickel-Pyrex	0.164
Nickel-Soda Glass	0.203
Gold-Pyrex	0.103
Gold-Soda Glass	0.128
Nichrome-Quartz	0.00236

Table 2/

Table 2

Calculation of the Instantaneous Stagnation-Point Heat Transfer to Model 2C in Run 275 at t = 150 Microseconds

From Trace Fig.4(b) $E(t) = 79.9$ millivolts

τ	$E(\tau)\times10^3$	$E(t)-E(\tau)\times10^3$	$(t-\tau)^{\frac{3}{2}}\times10^9$	$\frac{E(t)-E(\tau)}{(t-\tau)^{\frac{3}{2}}}\times10^6$
0	20.2	59.7	1837	0.032
2	22.8	57.1	1801	0.032
6	28.4	51.5	1728	0.030
8	30.4	49.5	1692	0.029
10	31.3	48.1	1656	0.029
20	36.8	43.1	1482	0.029
30	40	39.9	1314	0.030
40	43.6	36.3	1154	0.031
50	48.4	31.5	1000	0.032
60	53.2	26.7	853.8	0.031
70	56.7	22.2	715.5	0.031
80	59.7	20.2	585.7	0.034
90	61.3	18.1	464.8	0.039
100	65	14.9	353.6	0.042
105	66	13.9	301.9	0.046
110	68.3	11.6	253.0	0.046
115	71	8.9	207.1	0.043
120	73	6.9	164.3	0.042
125	74	5.9	125.0	0.047
130	74.2	5.7	89.44	0.064
135	75	4.9	58.09	0.084
140	76.5	3.4	31.62	0.108

From Fig.4(b) $\frac{E(t)}{\sqrt{t}} = \frac{79.9}{\sqrt{150}} = 6.52$ volts-sec units

From Fig.4(d) Integral = 7.08 volts-sec units

Thus $\dot{q}(150)$ = Model constants $\times \left[\frac{2E(t)}{\sqrt{t}} + \text{Integral}\right]$

= 3.57 Kw/cm^2

HBF

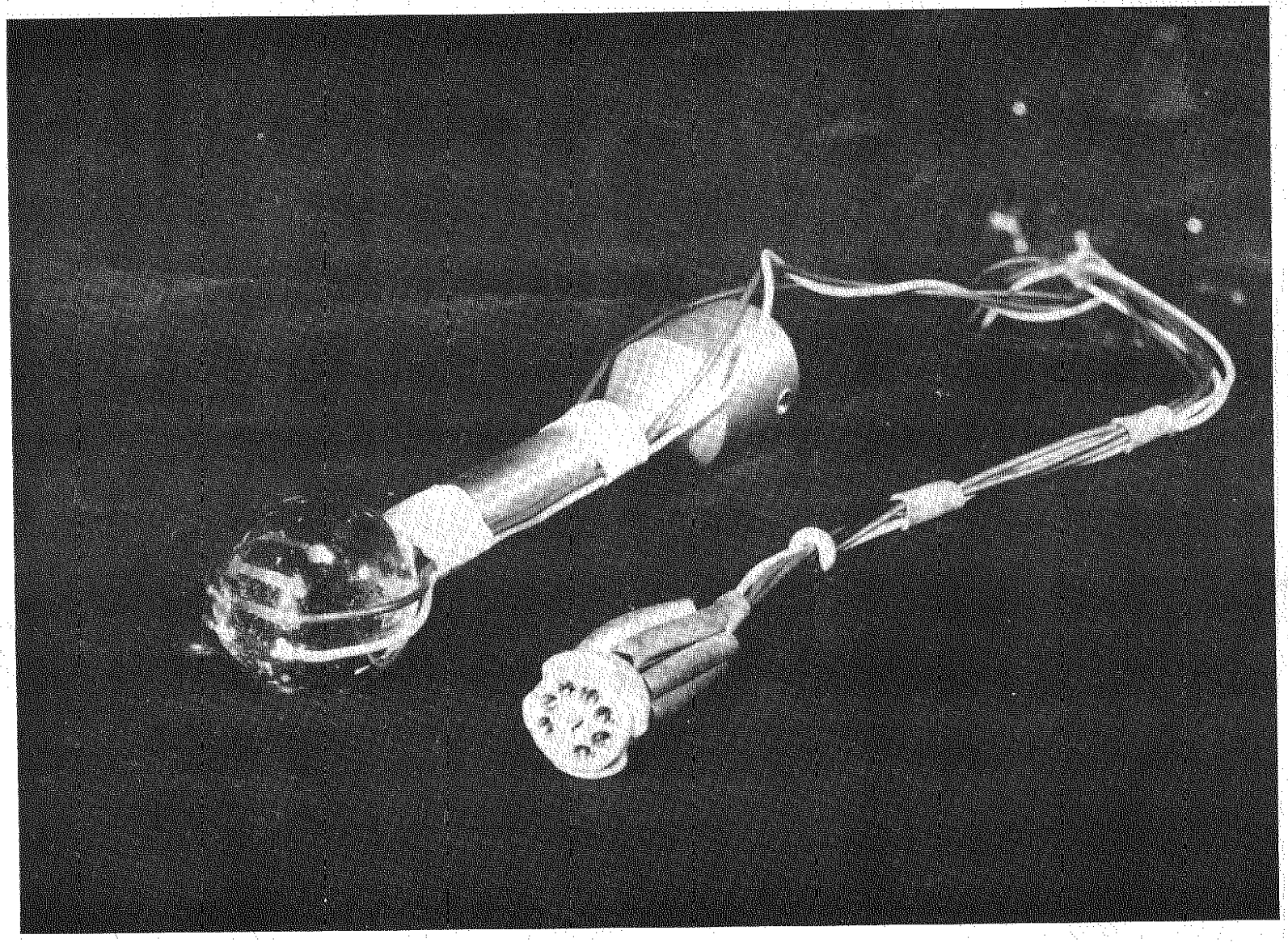

NPL THIN FILM RESISTANCE THERMOMETER HEAT TRANSFER MODEL

FIG. 1.

FIG. 2.

SPECIMEN HEAT TRANSFER MODEL CALIBRATION SHEET

DATE	12 / 4 / 58	SURFACE AREA A	0·050 cm^2
MODEL No	53	METHOD	PHOTO+PLANIMETER
TYPE	SPHERE	CRO	TEKTRONIX 545
SIZE	3/4 INCH	PRE AMP	53/54B
MATERIAL	SODA GLASS	V SENS	100mV/cm
SOURCE	ENGLISH GLASS C°.	H SENS	50μS/cm
SHOCK TUBE	3"	FILM MATERIAL	05 HANOVIA
LOCATION	——	CALIBRATION	FIRST

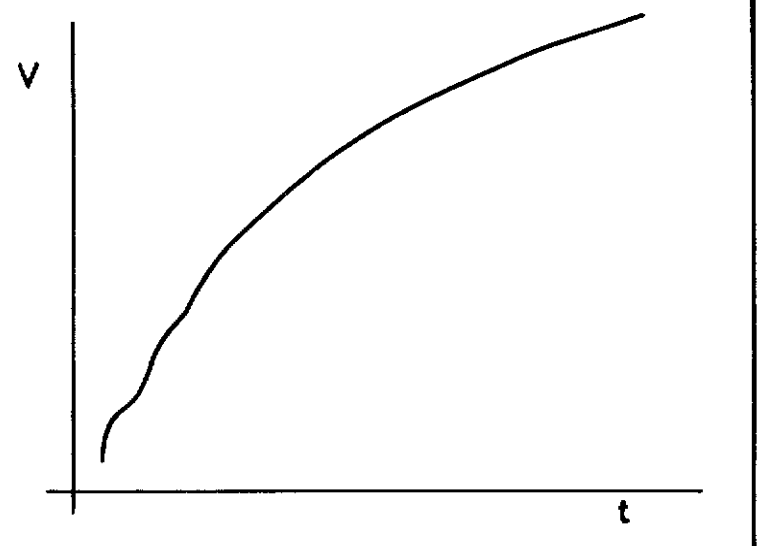

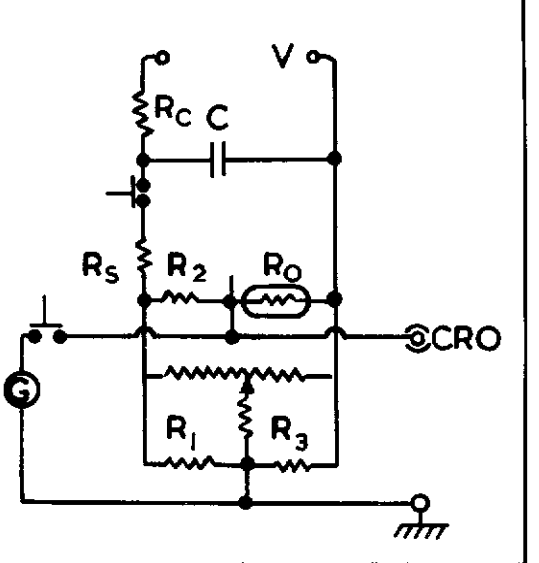

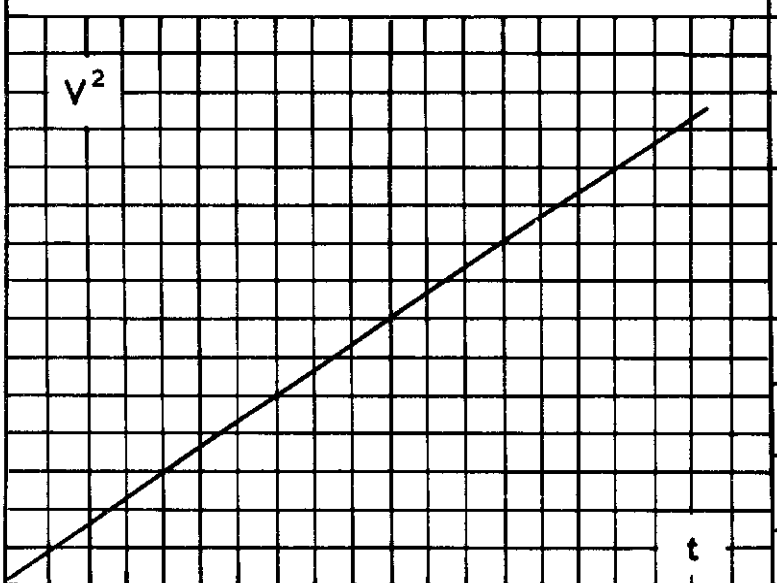

V VOLTS	250
C μF	250
R_C Ω	2,200
R_S Ω	200
$R_1=R_2=R_3$ Ω	58
R_O Ω	89
R_O METHOD	Avo

$\frac{\Delta V}{\sqrt{t}} \cdot A$	$\frac{3.72}{V^3}$	$\left(R_O+58+(R_O+174)\frac{R_S}{116}\right)^3$		$\frac{(R_O+58)}{58\,R_O^2}$	$\frac{a}{\sqrt{K\rho C}}$ $\frac{cm^2\,sec^{\frac{1}{2}}}{cals}$
1·176	$0·238\times10^{-6}$	$(600·4)^2$	216,400,000	0·00032	0·02
FROM FIG. 3					

FIG. 3(a & b).

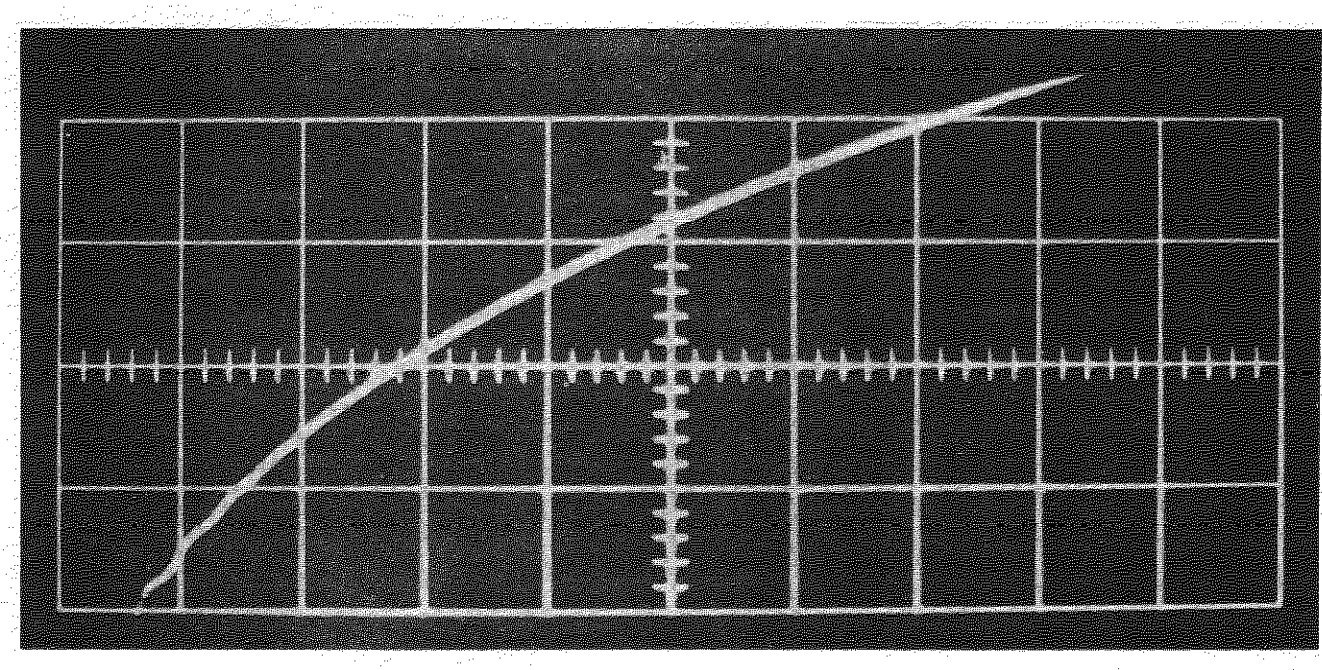

(a) CALIBRATION TRACE FOR MODEL 53
50 μsec / cm HORIZONTAL SCALE
100mV/ cm VERTICAL SCALE

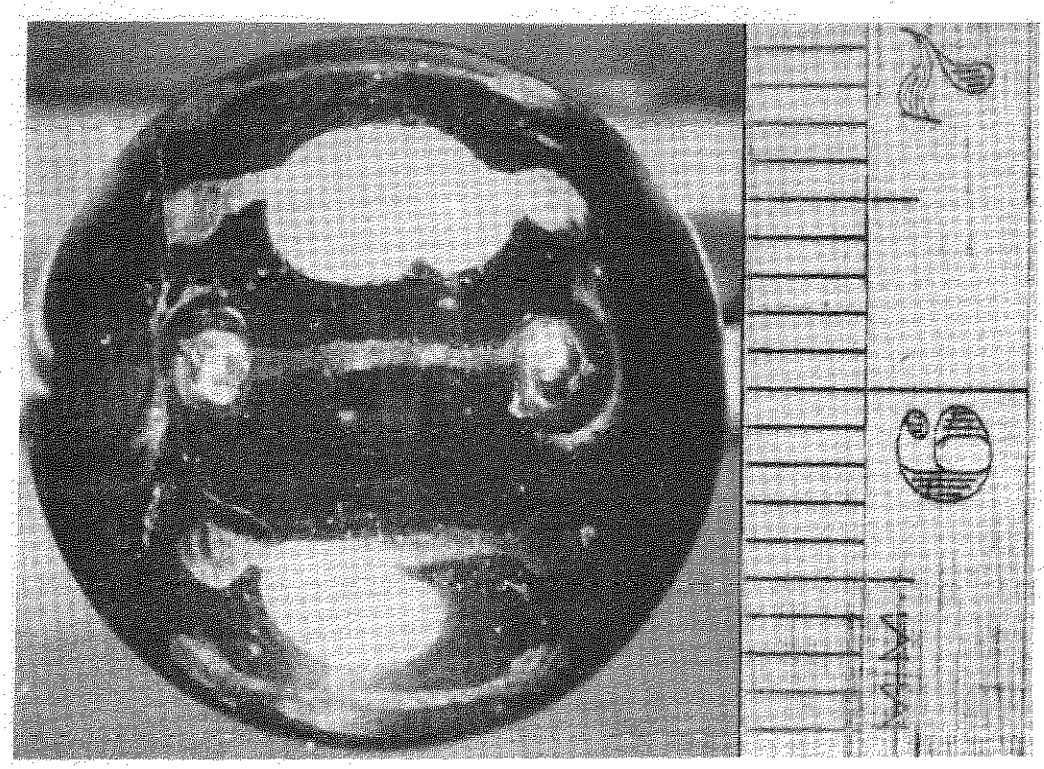

(b) PHOTOGRAPH OF MODEL 53 AND SCALE AT SAME MAGNIFICATION.

Fig. 3 c.

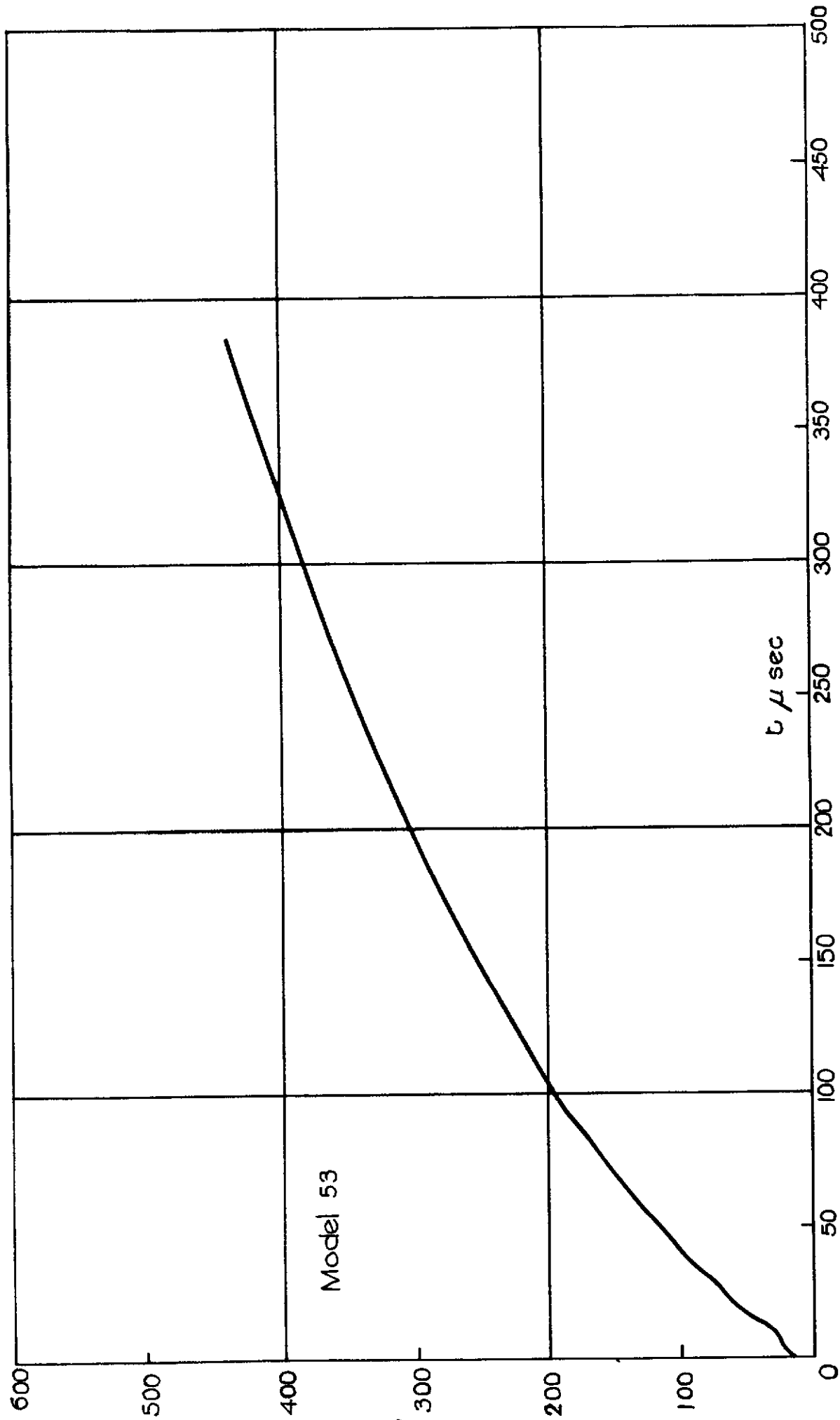

From oscilloscope trace
Calibration of heat transfer model.

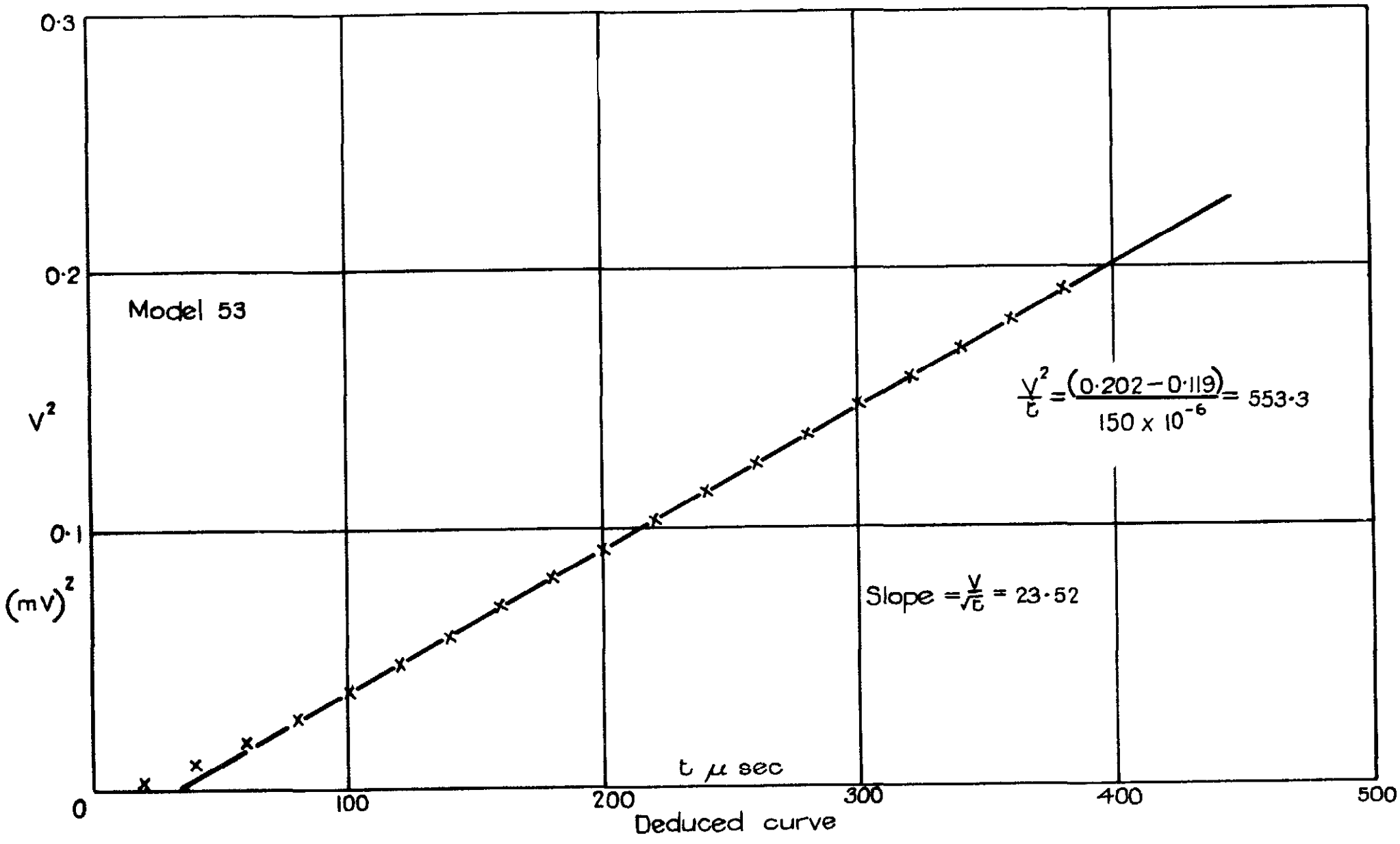

Fig. 3d

Calibration of heat transfer model

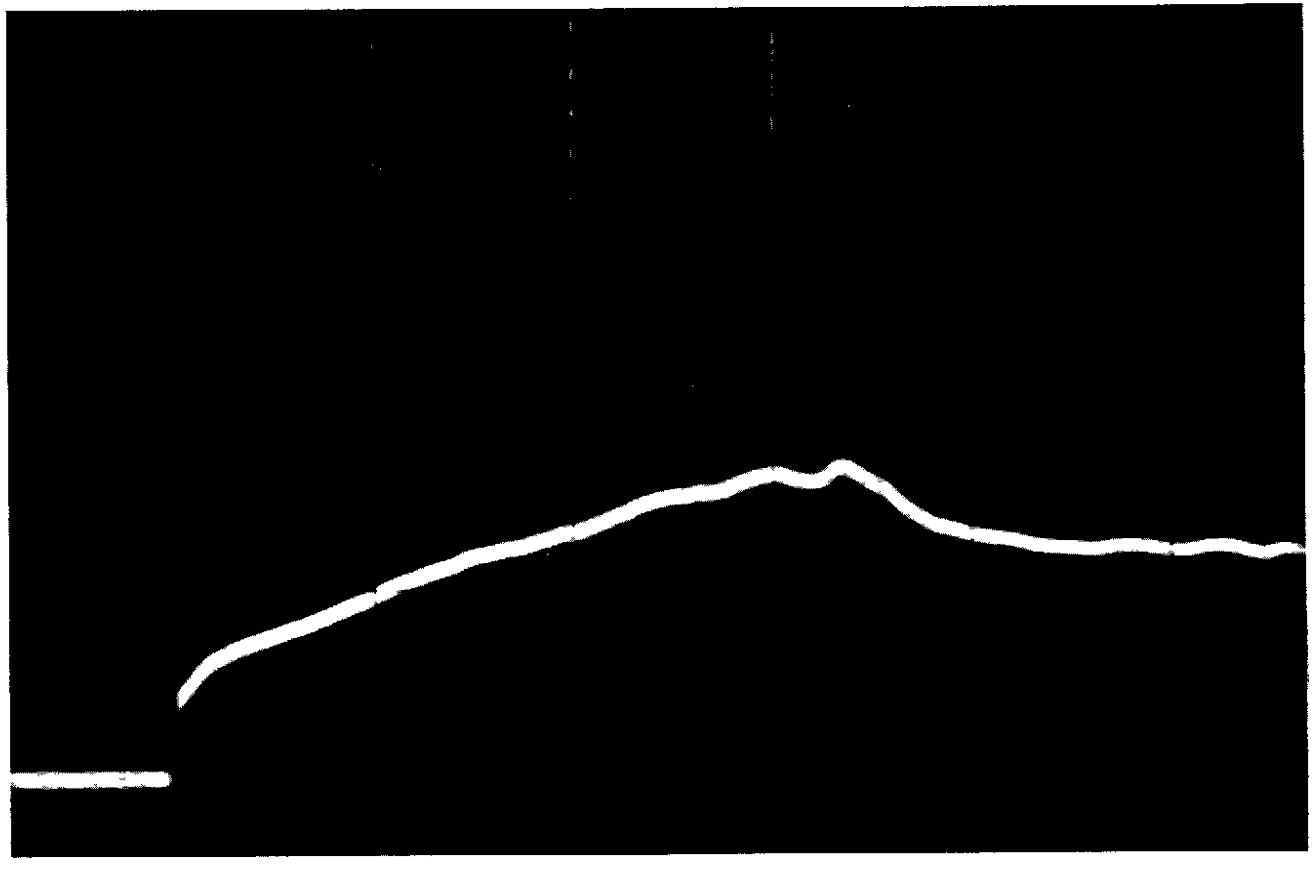

FIG. 4(a).

(a) RUN 273—MODEL 26. STAGNATION POINT RESISTANCE THERMOMETER OSCILLOSCOPE TRACE

50 μ sec / cm HORIZONTAL SCALE
50 mV / cm VERTICAL SCALE

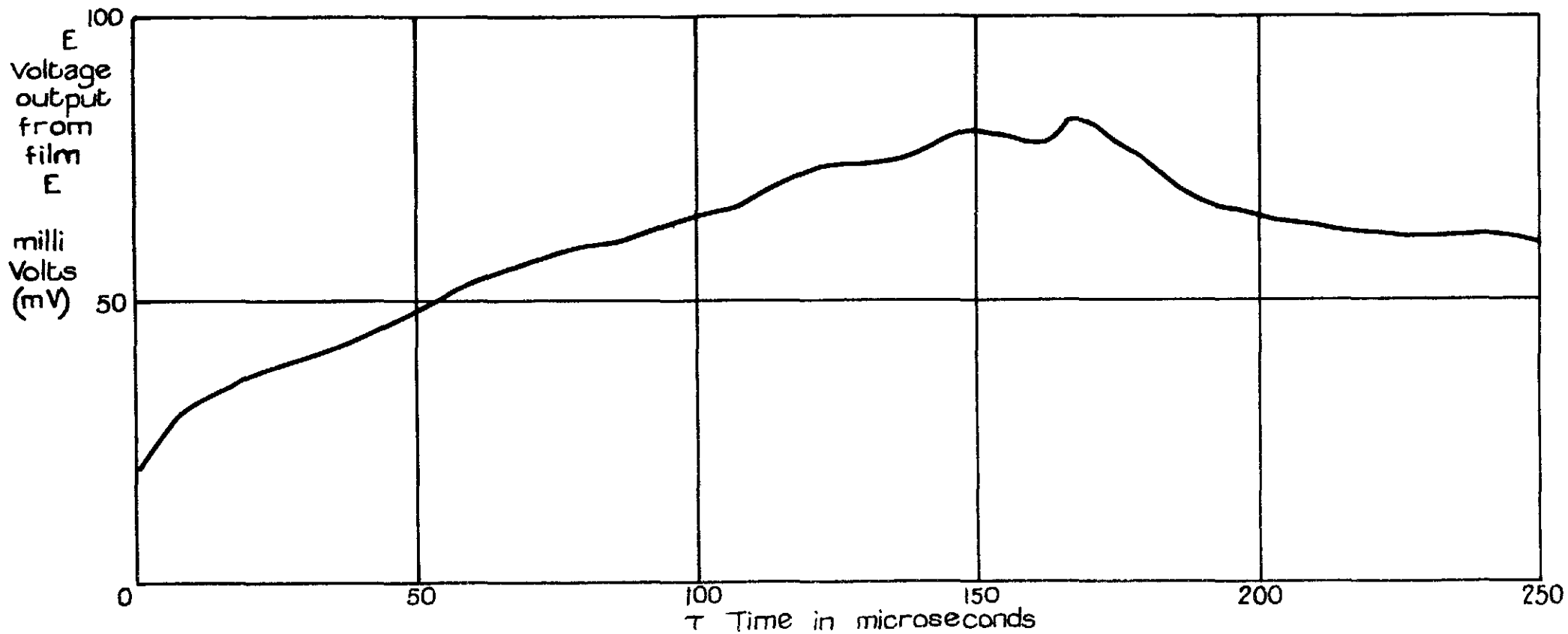

From oscilloscope record.

Analysis of heat transfer data from run 273 —— model 26

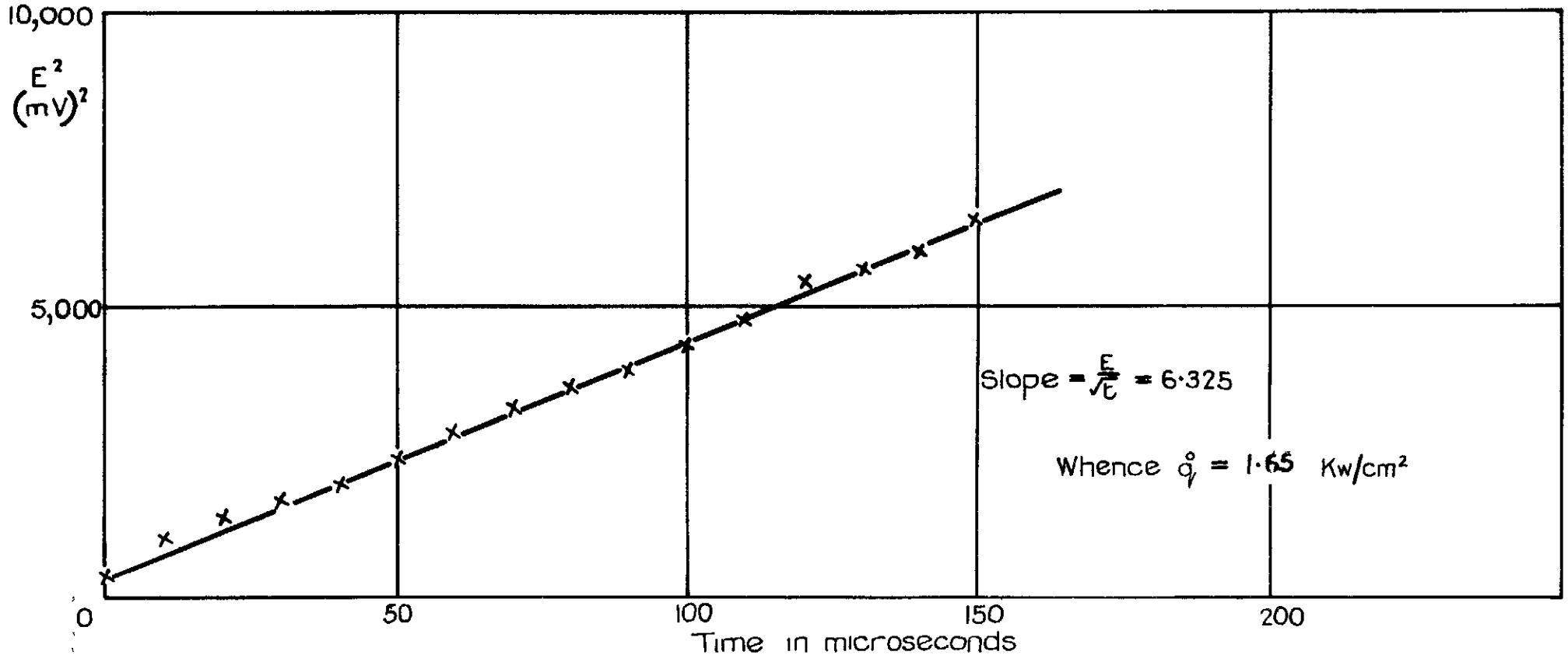

Constant heat transfer analysis

Analysis of heat transfer data from run 273—model 26

Fig. 4c

Fig, 4 d.

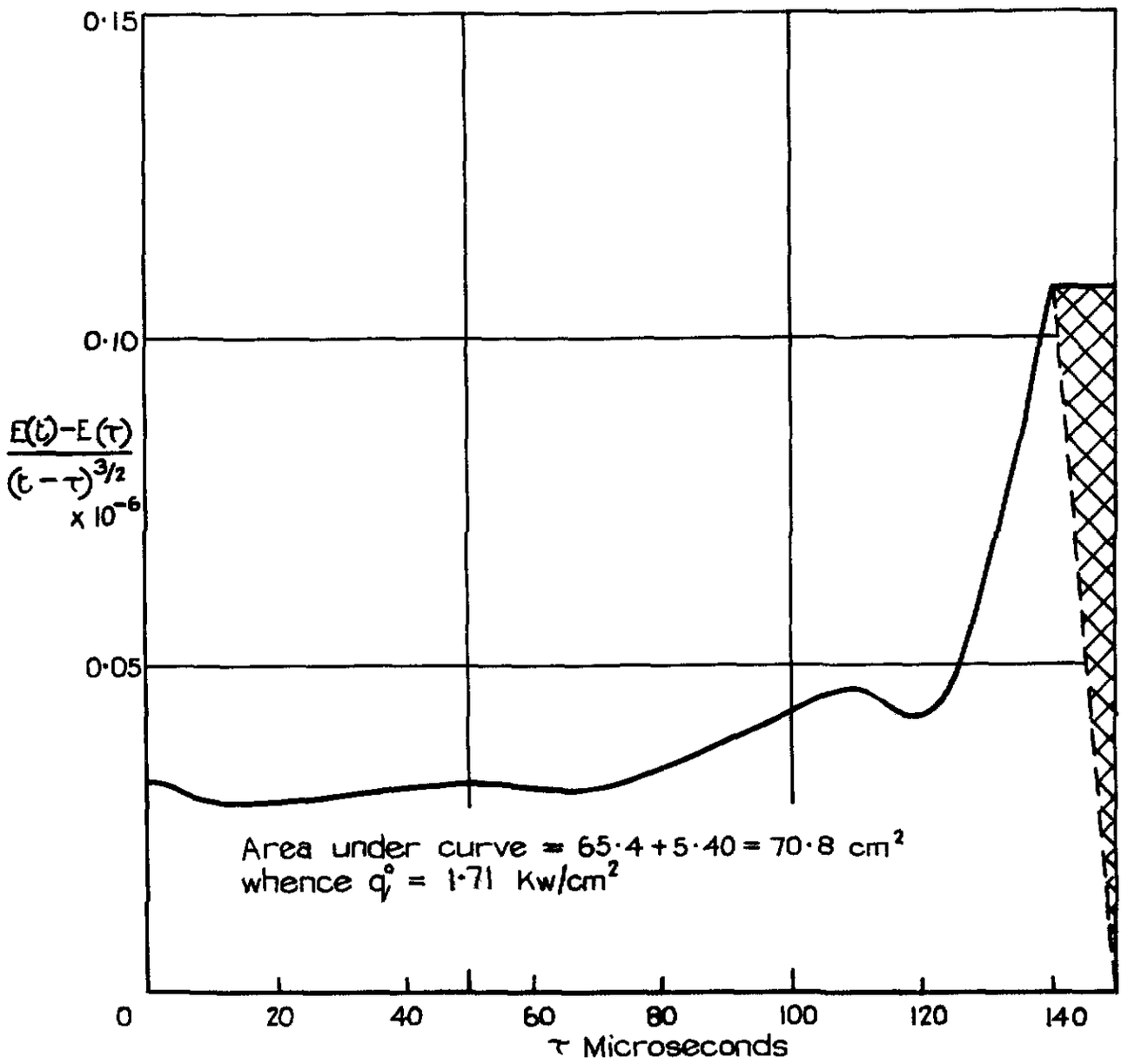

Evaluation of the instantaneous heat transfer rate at t = 150 microsec.

Run 273 — model 26 see table II

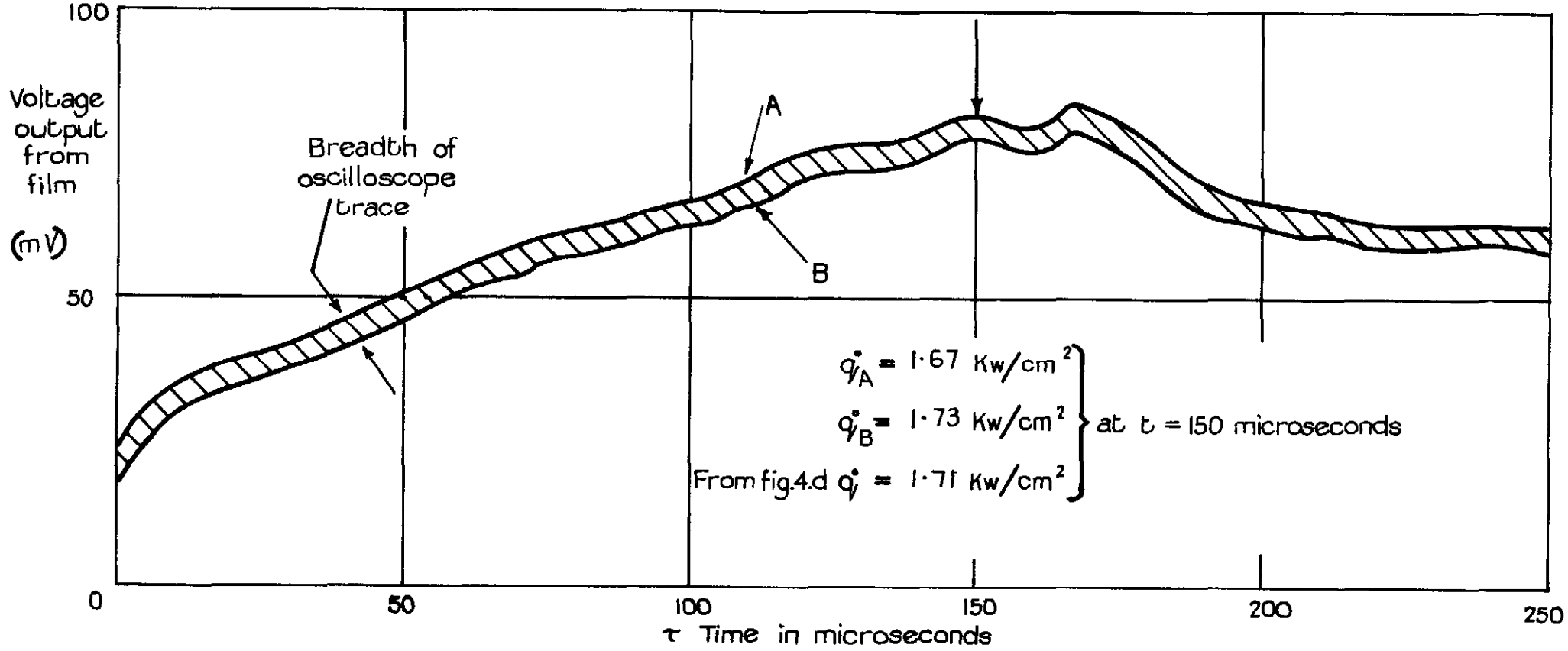

Run 273 — tracing errors.

Fig. 4.e.

C.P. No. 408
(20,204)
A.R.C. Technical Report

Printed and published by
HER MAJESTY'S STATIONERY OFFICE

To be purchased from
York House, Kingsway, London W.C.2
423 Oxford Street, London W.1
13A Castle Street, Edinburgh 2
109 St Mary Street, Cardiff
39 King Street, Manchester 2
Tower Lane, Bristol 1
2 Edmund Street, Birmingham 3
80 Chichester Street, Belfast
or through any bookseller

Printed in Great Britain

S O Code No 23-9011-8

C.P. No. 408